



Zero-obliquity twin lattice quasi-symmetry threefold twinning in 1- $\{(R)$ -1-[(3-oxo-2-isoindolinoyl)methyl]-2-propenyl}-5-methyl-2,3-indolinedione

Massimo Nespolo, Rebecca W. Smaha and Sean Parkin

Acta Cryst. (2020). B76, 643–649



IUCr Journals

CRYSTALLOGRAPHY JOURNALS ONLINE

Copyright © International Union of Crystallography

Author(s) of this article may load this reprint on their own web site or institutional repository provided that this cover page is retained. Republication of this article or its storage in electronic databases other than as specified above is not permitted without prior permission in writing from the IUCr.

For further information see <https://journals.iucr.org/services/authorrights.html>

Zero-obliquity twin lattice quasi-symmetry three-fold twinning in 1-*{(R)-1-[(3-oxo-2-isoindolinoyl)methyl]-2-propenyl}-5-methyl-2,3-indolinedione*

Massimo Nespolo,^{a*} Rebecca W. Smaha^b and Sean Parkin^c

^aUniversité de Lorraine, CNRS CRM2, Nancy, France, ^bDepartment of Chemistry, Stanford University, Stanford, CA 94305, USA, and ^cDepartment of Chemistry, University of Kentucky, Lexington, KY 40506, USA. *Correspondence e-mail: massimo.nespolo@univ-lorraine.fr

Received 17 April 2020

Accepted 15 June 2020

Edited by M. Dusek, Academy of Sciences of the Czech Republic, Czech Republic

Keywords: twinning; zero-obliquity twin lattice quasi-symmetry; twin misfit; chromatic symmetry.

Supporting information: this article has supporting information at journals.iucr.org/b

Threefold twinning in 1-*{(R)-1-[(3-oxo-2-isoindolinoyl)methyl]-2-propenyl}-5-methyl-2,3-indolinedione*, C₂₁H₁₆N₂O₄, has been reported recently [Trost *et al.* (2020). *Org. Lett.* **22**, 2584–2589] but the twin characterization was not published. This twinning presents several interesting features. The crystal structure is monoclinic, but its lattice is metrically strongly pseudo-orthorhombic and underpins a strongly pseudo-hexagonal sublattice. Several possible twin laws are compatible with these metric specializations, among which the one found experimentally corresponds to a trichromatic point group. Twinning is by reticular pseudo-merohedry with twin index 2 and zero obliquity but a non-zero twin misfit. The twin lattice coincides with the pseudo-hexagonal sublattice of the individual domain, which justifies the adoption of the unconventional setting $B2_1$ of the space group.

1. Introduction

During an investigation of ruthenium-catalysed asymmetric allylic alkylation of isatins, Trost *et al.* (2020) reported a number of compounds, among which 1-*{(R)-1-[(3-oxo-2-isoindolinoyl)methyl]-2-propenyl}-5-methyl-2,3-indolinedione* occurred as a three-individual twin. The crystal structure was solved and refined from the twinned sample [Cambridge Structural Database (CSD; Groom *et al.*, 2016) code WUGLES, deposition number 1981346], but full details of the twin were not reported. Here we provide a complete description of this twin.

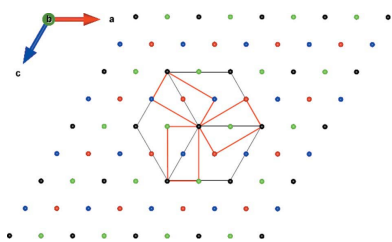
1-*{(R)-1-[(3-Oxo-2-isoindolinoyl)methyl]-2-propenyl}-5-methyl-2,3-indolinedione*, empirical formula C₂₁H₁₆N₂O₄, crystallizes in a monoclinic space group of type $P2_1$, No. 4 in Vol. A of the *International Tables for Crystallography* (2016). The conventional unit cell has cell parameters $a = 7.8146$ (6), $b = 49.062$ (2), $c = 13.5069$ (4) Å, $\beta = 89.955$ (5)° and $V = 5178.5$ (5) Å³ and presents strong pseudo-symmetry of two types:

(i) A strong orthorhombic pseudo-symmetry, due to the almost right β angle;

(ii) A strong hexagonal pseudo-symmetry, due to the ratio $c/a \simeq \tan(60^\circ)$ of the B -centred cell.

Because higher symmetry of the lattice or of a small sublattice is a pre-requisite for twinning (Nespolo, 2015), several twin laws could occur in a sample with these cell metrics (chromatic symmetry notation after Nespolo, 2019):

(i) Inversion twinning, leading to a two-individual twin with dichromatic twin point group $\mathcal{K}^{(2)} = 2/m'$;



© 2020 International Union of Crystallography

Table 1
 Experimental details†.

Crystal data	
Chemical formula	C ₂₁ H ₁₆ N ₂ O ₄
<i>M_r</i> (Mg m ⁻³)	2162.14
Crystal system, space-group type	Monoclinic, <i>B</i> ₂₁ (unconventional setting of <i>P</i> ₂₁ , No. 4)
Temperature (K)	100
<i>a</i> , <i>b</i> , <i>c</i> (Å)	15.5993 (8), 49.062 (2), 15.6099 (8)
β (°)	119.896 (2)
<i>V</i> (Å ³)	10357.0 (9)
<i>Z</i>	24
Radiation type	Cu <i>K</i> α
μ (mm ⁻¹)	0.80
Crystal size (mm)	0.68 × 0.07 × 0.07
Data collection	
Diffraction	D8 Venture with a PHOTON-II detector
Absorption correction	Multi-scan. <i>SADABS2016/2</i> (Bruker, 2016) was used for absorption correction. <i>wR</i> ₂ (int) was 0.1413 before and 0.0816 after correction. The ratio of minimum to maximum transmission is 0.6319. The $\lambda/2$ correction factor is not present.
<i>T</i> _{min} , <i>T</i> _{max}	0.208, 0.330
No. of measured, independent and observed [<i>I</i> > 2 σ (<i>I</i>)] reflections	349 707, 43 677, 39 928
<i>R</i> _{int}	0.058
(<i>sin</i> θ/λ) _{max} (Å ⁻¹)	0.639
Refinement	
<i>R</i> [<i>F</i> ² > 2 σ (<i>F</i> ²)], <i>wR</i> (<i>F</i> ²), <i>S</i>	0.044, 0.121, 1.08
No. of reflections	43 677
No. of parameters	1468
No. of restraints	1
H-atom treatment	H-atom parameters constrained
$\Delta\rho_{\max}$, $\Delta\rho_{\min}$ (e Å ⁻³)	0.21, -0.24
Absolute structure	Flack <i>x</i> determined using 9960 quotients [(<i>I</i> ⁺ - <i>I</i> ⁻)/(<i>I</i> ⁺ + <i>I</i> ⁻)] (Parsons <i>et al.</i> , 2013)
Absolute structure parameter	0.00 (5)

† Adapted from details given in the Supplementary Information of Trost *et al.* (2020). Computer programs: *APEX3* (Bruker, 2016), *SHELXD* (Sheldrick, 2008), *SHELXL* (Sheldrick, 2008), *OLEX2* (Dolomanov *et al.*, 2009).

(ii) Twofold-rotation about [100] (or [001]), leading to a two-individual twin with dichromatic twin point group $\mathcal{K}^{(2)} = 2'22'$;

(iii) Reflection about a plane normal to [100] (or [001]), leading to a two-individual twin with dichromatic twin point group $\mathcal{K}^{(2)} = m'2m'$;

(iv) Threefold-rotations about [010], leading to a three-individual twin with trichromatic twin point group $\mathcal{K}^{(3)} = 16^{(3)}1$ [unconventional *b*-unique setting of $6^{(3)}11$];

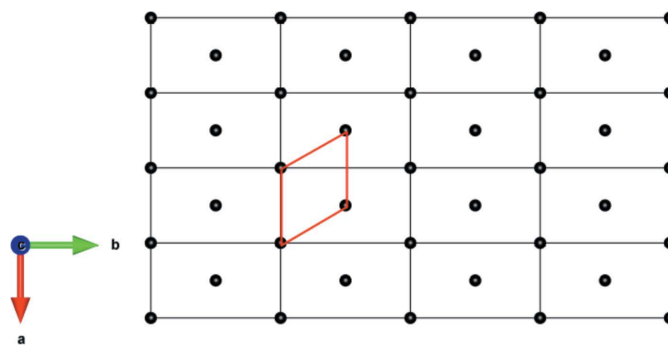
(v) Any combination of the four twin laws above, leading to a number of possibilities: a four-individual twin with quadrichromatic twin point group $\mathcal{K}^{(4)} = (2^{(2)}/m^{(2)}2/m^{(2)}2^{(2)}/m^{(2)})^{(4)}$; a six-individual twin with hexachromatic twin point group $\mathcal{K}^{(6)} = (2^{(2)}6^{(3)}2^{(2)})^{(6)}$ and unconventional *b*-unique setting of $(6^{(3)}2^{(2)}2^{(2)})^{(6)}$; a six-individual twin with hexachromatic twin point group $\mathcal{K}^{(6)} = (m^{(2)}6^{(3)}m^{(2)})^{(6)}$, an unconventional *b*-unique setting of $(6^{(3)}m^{(2)}m^{(2)})^{(6)}$; a six-individual twin with hexachromatic twin point group $\mathcal{K}^{(6)} = (6^{(3)}/m^{(2)})^{(6)}$; or a twelve-individual twin with dodecachromatic twin point group $\mathcal{K}^{(12)} = (2^{(2)}/m^{(2)}6^{(3)}/m^{(2)}2^{(2)}/m^{(2)})^{(12)}$, an unconventional *b*-unique setting of $(6^{(3)}/m^{(2)}2^{(2)}/m^{(2)}2^{(2)}/m^{(2)})^{(12)}$.

The compound was, however, enantiopure, which rules out all types of twin where the twin operations would be of the second kind (handedness inverting). The sample reported by Trost *et al.* (2020) corresponds to case (iv) above and represents a useful case study on how to solve and correctly characterize twins that are less straightforward.

2. Experimental

The synthesis has been described in detail by Trost *et al.* (2020) but the details of the structure refinement appeared only in the supplementary material. These are necessary for a complete description of the twin and we summarize them hereafter. A suitable crystal was selected under a polarizing microscope and diffraction data (100 K) were collected with Cu *K* α radiation on a Bruker D8 Venture diffractometer with a PHOTON-II detector. Data integration and reduction were performed with *SAINTE* and absorption correction with *SADABS* (Bruker, 2016). The structure was solved by the dual-space direct-methods program *SHELXD* (Sheldrick, 2008), which allows for the incorporation of two twin components. Least-squares minimization refinement of the three-component twin was carried out using the *SHELXL* refinement program (Sheldrick, 2008), called from within *OLEX2* (Dolomanov *et al.*, 2009). All non-hydrogen atoms were refined with anisotropic atomic displacement parameters. Atomic displacement parameters for the hydrogen atoms were tied to the equivalent isotropic displacement parameter of the atom to which they are bonded [*U*_{iso}(H) = 1.5*U*_{eq}(C) for methyl, 1.2*U*_{eq}(C) for all others]. The absolute structure was determined using resonant scattering from 9960 selected quotients (Parsons *et al.*, 2013) with *SHELXL* (Sheldrick, 2008). The Flack parameter of 0.00 (5) indicates that the crystal was enantiopure and the absolute structure was correct. Full experimental details, adapted from Trost *et al.* (2020), are given in Table 1.

To rule out the possibility of a six-individual twin with hexachromatic twin point group $\mathcal{K}^{(6)} = (2^{(2)}6^{(3)}2^{(2)})^{(6)}$, we


Figure 1

A hexagonal lattice seen in projection along [001]. The red unit cell is the conventional *hP* unit cell. This lattice can be described by an orthorhombic *C*-centred unit cell (black unit cells), which is known as an orthohexagonal unit cell. Its cell parameters in the (001) plane have the ratio *b/a* = tan (60°). This and Figs. 2, 3, 5, 6 and 7 were drawn using *VESTA* (Momma & Izumi, 2011).

repeated the refinement with *JANA2006* (Petříček *et al.*, 2014), which allows for multi-domain refinement, including six volume fractions to be refined. Three of these refined to zero, confirming that the twin is indeed trichromatic.

3. The twin lattice and the choice of the unconventional setting of the space group

Any hexagonal lattice can be described by an orthohexagonal *S*-centred unit cell with the ratio of cell parameters in the plane of the *S* face equal to $\tan(60^\circ) = 3^{1/2}$. *S*-centring is a standard general symbol to describe a single-face-centring: depending on whether the plane corresponding to this face is (100), (010) or (001), *S*-centring becomes *A*-, *B*- or *C*-centring, respectively. An orthorhombic lattice whose conventional unit cell is *S*-centred and whose ratio of cell parameters is close to $\tan(60^\circ)$ is *pseudo*-hexagonal (Fig. 2).

An orthorhombic lattice whose conventional unit cell is primitive and has two cell parameters in a ratio (almost) equal to $\tan(60^\circ)$ is not (pseudo)-hexagonal but has a (pseudo)-hexagonal sublattice¹. Some examples are known in the literature, like djurleite, with $\tan^{-1}(a/c) = 59.73^\circ$ (Takeda *et al.*, 1967), LiNH_4SO_4 , with $\tan^{-1}(a/b) = 59.97^\circ$ (Docherty *et al.*, 1988), $(\text{NH}_4)_2\text{SO}_4$ with $\tan^{-1}(b/c) = 60.85^\circ$ (Docherty *et al.*, 1988) and leadhillite, with $\tan^{-1}(b/c) = 60.89^\circ$ (Bindi & Menchetti, 2005). To emphasize this higher metric symmetry of a *sub*-lattice, one can adopt a non-standard setting of the space group (Nespolo & Aroyo, 2016) in which two of the three axes are not along the symmetry directions of the lattice but along the diagonal directions; the result is an *S*-centred unit cell that is metrically (pseudo)-hexagonal (Fig. 2). This is precisely the situation in $\text{C}_{21}\text{H}_{16}\text{N}_2\text{O}_4$, where:

(i) The pseudo-hexagonal axis is the *b* axis of the coordinate system, so that the ratio of cell parameters close to $\tan(60^\circ)$ is c/a ;

(ii) As a result of (i), the metrically pseudo-hexagonal cell is *B*-centred instead of *C*-centred;

(iii) The lattice is not exactly orthorhombic but only (strongly) pseudo-orthorhombic, and the symmetry of the underlying crystal structure is actually monoclinic.

The twin operations are the two threefold (120° and 240°) rotations about [010], and the twin lattice is the pseudo-hexagonal sublattice of nodes restored by these operations. These conditions correspond to the blue unit cell in Fig. 2, on which the axes permutation $(\mathbf{a}, \mathbf{b}, \mathbf{c}) \rightarrow (\mathbf{b}, \mathbf{c}, \mathbf{a})$ is performed to obtain the unique axis along **b**. Adopting the pseudo-hexagonal coordinate system defined by this sublattice corresponds to describing the individual in an unconventional setting of the space group, namely $B2_1$, in which the cell parameters become $a = 15.5993$ (8), $b = 49.062$ (2), $c = 15.6099$ (8) Å, $\beta = 119.896$ (2)° and $V = 10357.0$ (9) Å³. This is precisely the setting used by Trost *et al.* (2020).

¹ We remind the reader that a sublattice \mathbf{L}_s is obtained from an original lattice \mathbf{L} by removing some of the translations. The translation group of \mathbf{L}_s is a subgroup of the translation group of \mathbf{L} . The unit cell of \mathbf{L}_s is a supercell (larger volume) of the unit cell of \mathbf{L} .

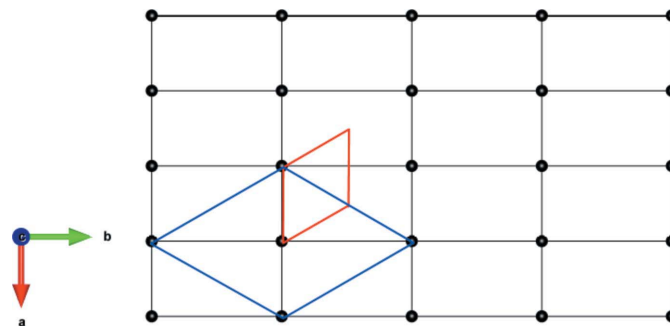


Figure 2

An orthorhombic lattice whose conventional unit cell is primitive, and whose cell parameters in the (001) plane have the ratio $b/a = \tan(60^\circ) = 3^{1/2}$, seen in projection along [001]. In this case, the red parallelogram is not a unit cell (only two of the corners correspond to lattice nodes), showing that the lattice is not hexagonal despite the metric specialization of the cell parameters. The blue parallelogram is, however, a unit cell: it is a supercell with twice the volume of the *oP* unit cell, which defines a hexagonal sublattice. With respect to the orthorhombic lattice, the blue unit cell is *C*-centred and non-conventional: its axes are along the [110], $[\bar{1}\bar{1}0]$ and [001] directions of the lattice; the two axes in the (001) plane are away from the symmetry directions of the lattice, [100] and [010].

4. Description of the twin law and the twin operations

A twin law is the set of equivalent twin operations obtained by decomposing the twin point group \mathcal{K} with respect to the intersection of the point groups of the individuals, $\mathcal{H}^* = \cap_i \mathcal{H}_i$ (Nespolo, 2019). In our case, the three individuals have their symmetry elements (the twofold rotation axis) parallel, so that $\mathcal{H}^* = \mathcal{H}_1 \cap \mathcal{H}_2 \cap \mathcal{H}_3 = \mathcal{H}_1 = \mathcal{H}_2 = \mathcal{H}_3 = 2$. The twin point group $\mathcal{K}^{(3)} = 16^{(3)}1$ therefore gives three cosets when decomposed with respect to \mathcal{H}^* because 2 being a normal subgroup of 6, left and right cosets coincide:

$$\begin{aligned} \mathcal{K}^{(3)} &= 16^{(3)}1 \\ &= \{1, 2_{[010]}\} \cup \left\{ 3_{[010]}^+, 6_{[010]}^- \right\}^{(2)} \cup \left\{ 3_{[010]}^-, 6_{[010]}^+ \right\}^{(2)}. \end{aligned} \quad (1)$$

The operations in each coset (twin law) are dichromatic because each operation taken individually relates two individuals; the chromaticity ⁽²⁾ is written outside the bracket collecting all the twin operations of a single twin law. The first coset is the point group of the individual, while the second and third cosets are the two twin laws, each of which contains two twin operations. We choose the threefold rotations as coset representatives. They are performed about the *b* axis and are represented by the following matrices, which are immediately obtained from the corresponding matrices of the conventional *c*-unique setting by the basis vectors permutation $(\mathbf{a}, \mathbf{b}, \mathbf{c}) \rightarrow (\mathbf{b}, \mathbf{c}, \mathbf{a})$:

$$3_{[010]}^+ = \begin{pmatrix} \bar{1} & 0 & 1 \\ 0 & 1 & 0 \\ \bar{1} & 0 & 0 \end{pmatrix}; \quad 3_{[010]}^- = \begin{pmatrix} 0 & 0 & \bar{1} \\ 0 & 1 & 0 \\ 1 & 0 & \bar{1} \end{pmatrix}. \quad (2)$$

However, the structure solution and refinement were performed with *SHELX* (Sheldrick, 2008), which requires that twin matrices be expressed with respect to the cell setting used

to describe the model. Thus, for the conventional (pseudo-*oP*) cell, the matrices would have to be expressed relative to an individual of the twin, rather than the twin itself. For the unconventional (pseudo-*hB*) cell, however, the unit cell of the twin lattice is coincident with the unconventional (pseudo-*hB*) cell of the first individual. For the pseudo-*oP* case, the matrices in equation (2) would have to be transformed with respect to the pseudo-*oP* unit cell. If \mathbf{P} is the transformation matrix corresponding to a change of reference (we can ignore a possible shift of the origin, which is of no concern in our case), the transformation from the matrix \mathbf{W}_1 representing an isometry in the first basis to the matrix \mathbf{W}_2 representing the same isometry in the second basis is simply

$$\mathbf{W}_2 = \mathbf{P}^T \mathbf{W}_1 \mathbf{P}, \quad (3)$$

where \mathbf{P}^T is the transpose of \mathbf{P} . The matrix \mathbf{P} is obtained by simple inspection of Fig. 2,

$$\mathbf{P} = \begin{pmatrix} 0.5 & 0 & -0.5 \\ 0 & 1 & 0 \\ 0.5 & 0 & 0.5 \end{pmatrix}, \quad (4)$$

which leads to

$$3_{[010]}^+ = \begin{pmatrix} -0.5 & 0 & 0.5 \\ 0 & 1 & 0 \\ -1.5 & 0 & -0.5 \end{pmatrix}; \quad 3_{[010]}^- = \begin{pmatrix} -0.5 & 0 & -0.5 \\ 0 & 1 & 0 \\ 1.5 & 0 & -0.5 \end{pmatrix}. \quad (5)$$

Although the nature of the operation is revealed by the determinant and trace of the matrices, which are invariant under a change of basis, the representation given in equation

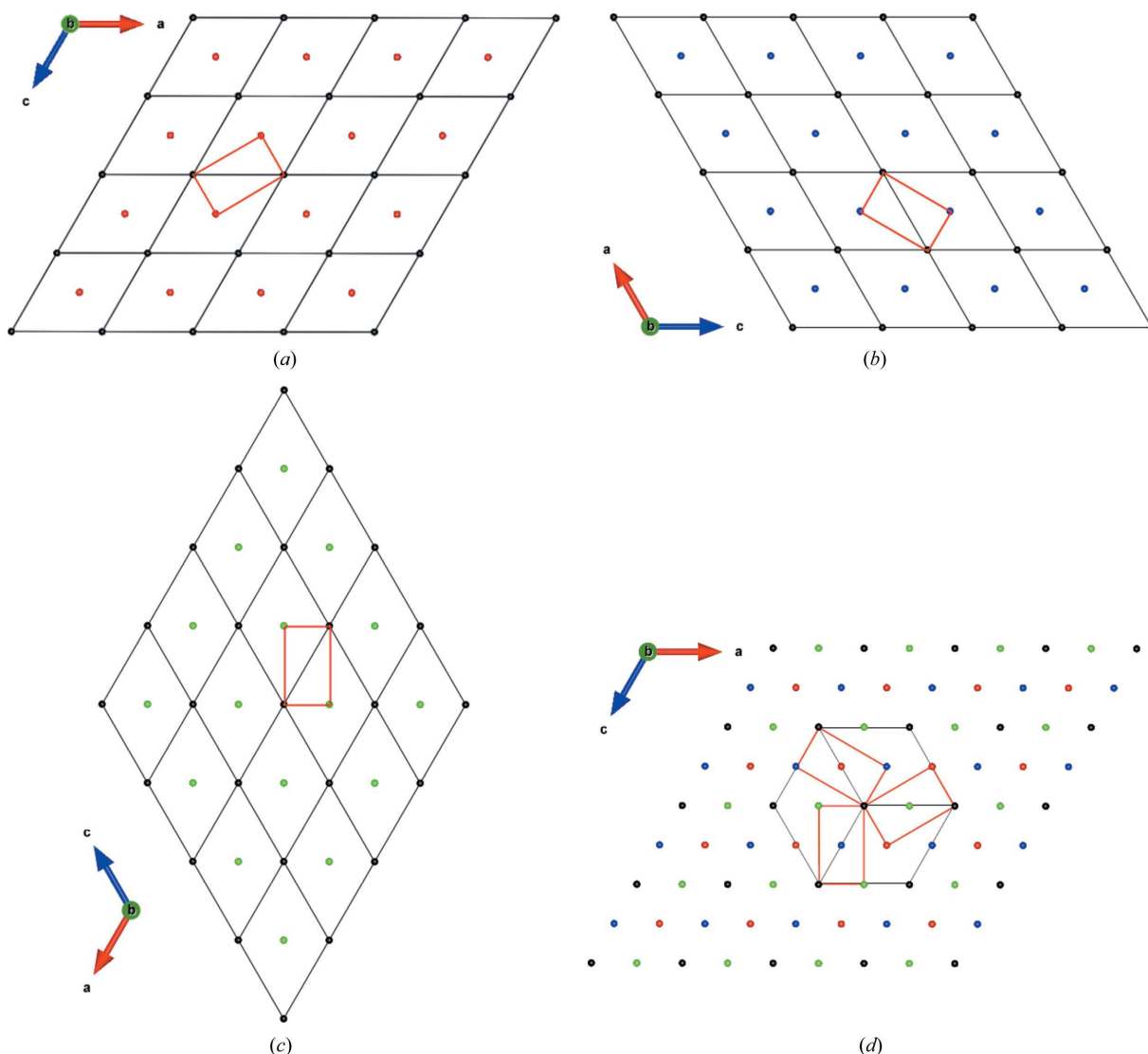


Figure 3 (a) A projection along [010] of the lattice of one individual of $C_{21}H_{16}N_2O_4$, indexed with respect to the pseudo-*hB* unit cell (black) and the pseudo-*oP* unit cell (red). The lattice nodes in red are those centring the pseudo-*hB* unit cell. (b) A projection along [010] of the lattice of the second individual, obtained by rotating that of the first individual 120° anticlockwise. The lattice nodes centring the pseudo-*hB* unit cell are now in blue. (c) A projection along [010] of the lattice of the third individual, obtained by rotating that of the first individual 240° anticlockwise. The lattice nodes centring the pseudo-*hB* unit cell are now in green. (d) An overlay of (a), (b) and (c). Half of the lattice nodes are restored, so that the twin index is 2.

(2) is intuitive to read, in contrast to representation (5). For this reason, from a practical standpoint, the representation in the basis of the twin lattice is always preferable, despite the requirements imposed by some software (Nespolo, 2016).

5. Characterization of twinning

For the characterization of twinning, two parameters are usually specified: the twin index and the obliquity. The twin index is the inverse of the fraction of lattice nodes restored by the twin operation, and corresponds to the ratio of the volume of the primitive unit cells of the twin lattice and of the individual lattice. The obliquity measures the deviation from the exact overlap of lattice nodes but it is often insufficient in cases of multiple twinning. In the present case, the twin lattice has a pseudo-*hP* unit cell whose volume is twice that of the *mP* unit cell of the individual. The twin index is therefore 2. This can also be verified graphically.

Fig. 3(*a*) shows the projection along [010] of the lattice of one individual, indexed with respect to the pseudo-*hB* unit cell (black). The lattice nodes centring the pseudo-*hB* unit cell are shown in red. The pseudo-*oP* unit cell is also shown in red. Fig. 3(*b*) is obtained by rotating Fig. 3(*a*) 120° anticlockwise and corresponds to the second individual; the lattice nodes centring the pseudo-*hB* unit cell are now in blue. Fig. 3(*c*) is obtained by rotating Fig. 3(*a*) 240° anticlockwise and corresponds to the third individual. The lattice nodes centring the pseudo-*hB* unit cell are now in green. For each of the three individuals, the node at the origin (black node) is in common

(restored by the twin operation), whereas the node centring the plane (coordinates $\frac{1}{2}, 0, \frac{1}{2}$) is not, so that the twin index is $2/1 = 2$. Fig. 3(*d*) is obtained by overlapping Figs. 3(*a*), 3(*b*) and 3(*c*). The metrically pseudo-hexagonal cells (black) each contain two lattice nodes which, in the axial setting of the twin, have coordinates $0, 0, 0$ and $\frac{1}{2}, 0, \frac{1}{2}$ (black and red), $0, 0, 0$ and $\frac{1}{2}, 0, 0$ (black and green), and $0, 0, 0$ and $0, 0, \frac{1}{2}$ (black and blue).

Twinning has been broadly classified into TLS (twin lattice symmetry) and TLQS (twin lattice quasi-symmetry), depending on whether or not the twin operation leads to exact overlap of the lattice nodes (Donnay & Donnay, 1974). Fig. 3 is drawn without taking into account the slight divergence from exact hexagonal metric of the unit cells, *i.e.* as in TLS. Because the unit cells are actually only pseudo-hexagonal, this twin corresponds to TLQS, and the twin operations result in a slight divergence from exact overlap of lattice nodes. In TLQS, the divergence from exact lattice overlap is usually measured by the obliquity, which is defined as the angular deviation from exact perpendicularity of the twin axis and a lattice plane (for rotation twins) or of the twin plane and a lattice direction (for reflection twins). The obliquity is sufficient to characterize TLQS in twofold twins. In the present case, the twin operation is a threefold rotation and the twin axis, [010], is exactly perpendicular to the lattice plane (010). The obliquity is therefore zero, yet the twinning is TLQS. It is precisely to characterize this type of twinning that Nespolo & Ferraris (2007) introduced the notion of *twin misfit* as the distance between the two closest lattice nodes belonging to the lattices of twinned individuals. In our case, the twin misfit is calculated as the difference between the 010 lattice node of one individual and the position obtained by applying a 120° anticlockwise rotation to the 100 lattice node of another individual. By applying the cosine rule, one obtains $[15.6099^2 + 15.5993^2 - 2 \times 15.6099 \times 15.5993 \cos(120 - 119.896)^\circ]^{1/2} = 0.011 \text{ \AA}$. The same result is obtained by taking any equivalent pair of nodes, *e.g.* $\bar{1}10$ versus 010 rotated 120° anticlockwise, or 100 versus $\bar{1}10$ rotated 120° anticlockwise. Twinning is therefore by reticular pseudo-merohedry (TLQS with twin index > 1). Fig. 4 shows a reciprocal-space-slice image of the

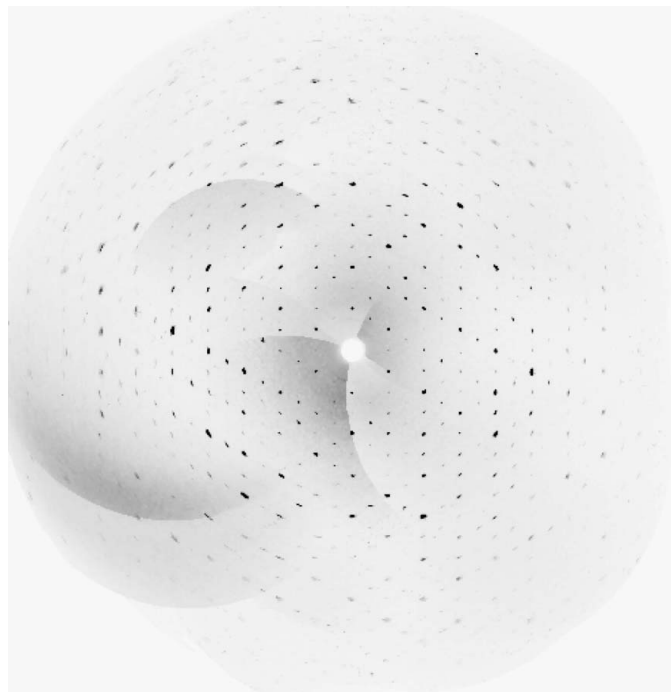


Figure 4

A reciprocal-space-slice image of the $(h0l)^*$ plane. At higher diffraction angles the reflections are slightly elongated arcs, consistent with the non-zero twin misfit.

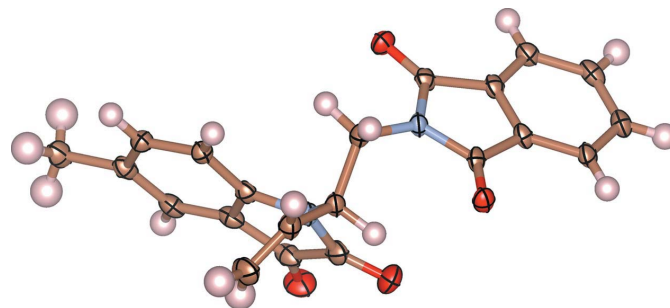


Figure 5

A displacement ellipsoid plot (50% probability level) of a single $C_{21}H_{16}N_2O_4$ molecule. Red, lavender, chocolate and light pink represent oxygen, nitrogen, carbon and hydrogen atoms, respectively. The molecular structure gives no reason to suspect twinning in the crystal.

($h0l$)* plane. At higher diffraction angle the reflections are slightly elongated arcs, consistent with the non-zero twin misfit.

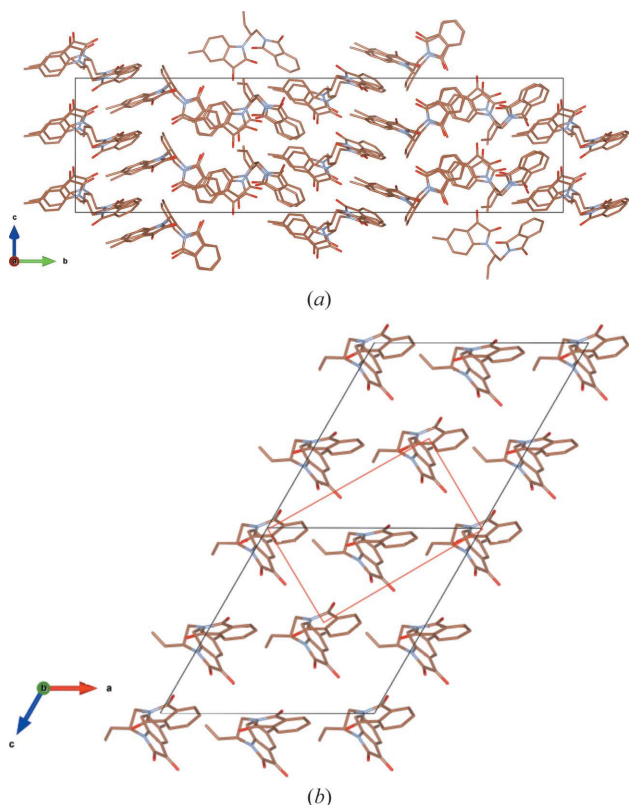


Figure 6
A wireframe view of the molecular packing of $C_{21}H_{16}N_2O_4$, (a) along [001] and (b) along [010] (section to $0.05b$ and hydrogen atoms removed to improve readability). The black and red unit cells in (b) are pseudo- hB and pseudo- oP , respectively.

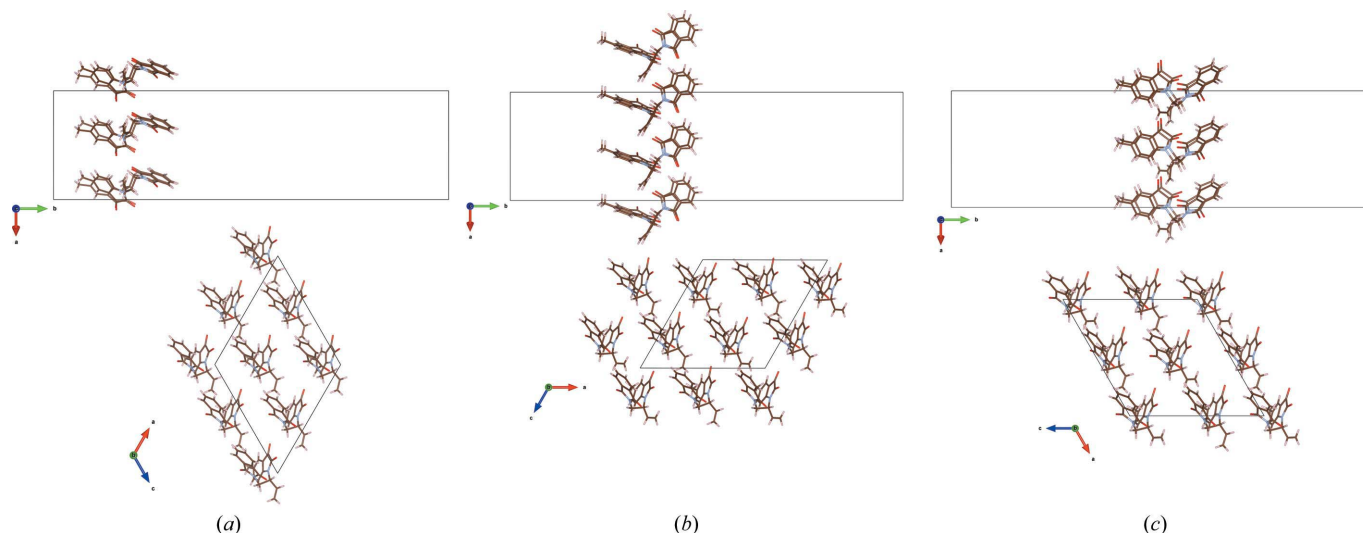


Figure 7
The structure of $C_{21}H_{16}N_2O_4$, sliced into three layers approximately $b/6$ apart. The unit cells in the top part of each panel are seen along [001] and have the same orientation, whereas in the bottom part they are seen along [010] and are rotated 60° from each other. In these respective orientations, the three layers are approximately parallel. The figure shows the existence of a pseudo- 6_1 screw rotation along [010], of which only the $6_1^3 = 2_1$ is exactly realized.

6. Discussion

Fig. 5 shows the molecule in a ball-and-stick representation. Fig. 6 shows the molecular packing, (a) along [001] and (b) along [010].

The asymmetric unit of the structure comprises six molecules arranged in three distinct layers. Fig. 7 shows these layers. The top of the figure represents the pseudo- hB (b -unique setting) unit cell seen along [001]: the three layers are separately shown in panels (a), (b) and (c) of the figure and are approximately $b/6$ apart. The three other layers related by the 2_1 screw axis are not shown, to improve readability of the figure. The bottom of the figure shows the same representation, this time along [010], *i.e.* the symmetry axis of the structure. The unit cells in panels (a), (b) and (c) are rotated 60° from each other. In these respective orientations, the three layers are approximately parallel. The structure therefore shows a pseudo- 6_1 screw rotation along [010], of which only the $6_1^3 = 2_1$ is exactly realized. By imposing the exact 6_1 symmetry, one would obtain a higher-symmetry phase, which might correspond to an ideal prototype or possibly a high-temperature phase. Whether this phase really exists in the temperature range in which the compound is stable is not known. Nevertheless, the twin operations correspond to the linear part of the pseudo-screw rotations, suggesting that the pseudo-symmetry of the structure is probably the structural reason for twinning.

7. Conclusions

Twinning is often considered a disturbing phenomenon that hinders the routine of structure solution and refinement. It is not uncommon that, when a new structure is reported from a twinned sample, the details of the twinning are incompletely characterized or even left out of the report, possibly obscured in the supplementary material. Nonetheless, twinning is

actually a phenomenon of profound importance for materials science, structural science and the physics of crystal growth, as shown by the huge and constantly increasing literature on twinning. A thorough characterization of a twinned sample, however, often goes beyond routine work, especially when less straightforward cases occur. We hope that the analysis presented here will be useful as a guideline for further detailed characterizations of twinned samples.

Acknowledgements

We are especially grateful to Professor B. M. Trost (Stanford University) for the opportunity to work on such a fascinating specimen, and in particular to Dr C. A. Kalnmals, D. Ramakrishnan and Dr M. C. Ryan, who synthesized the compound and grew the crystals. We would also like to thank C. M. Galvin, who aided with data collection. Comments from two anonymous reviewers are gratefully acknowledged.

Funding information

Part of this work was performed at the Stanford Nano Shared Facilities (SNSF), supported by the US National Science Foundation under award ECCS-1542152.

References

- Bindi, L. & Menchetti, S. (2005). *Am. Mineral.* **90**, 1641–1647.
- Bruker (2016). *APEX3* (Version 2016.9-0) and *SADABS2016/2*. Bruker AXS Inc., Madison, Wisconsin, USA.
- Docherty, R., El-Korashy, A., Jennissen, H.-D., Klapper, H., Roberts, K. J. & Scheffen-Lauenroth, T. (1988). *J. Appl. Cryst.* **21**, 406–415.
- Dolomanov, O. V., Bourhis, L. J., Gildea, R. J., Howard, J. A. K. & Puschmann, H. (2009). *J. Appl. Cryst.* **42**, 339–341.
- Donnay, G. & Donnay, J. D. H. (1974). *Can. Mineral.* **12**, 422–425.
- Groom, C. R., Bruno, I. J., Lightfoot, M. P. & Ward, S. C. (2016). *Acta Cryst.* **B72**, 171–179.
- International Tables for Crystallography* (2016). Vol. A, *Space-group symmetry*, edited by M. I. Aroyo. Chichester: Wiley.
- Momma, K. & Izumi, F. (2011). *J. Appl. Cryst.* **44**, 1272–1276.
- Nespolo, M. (2015). *Cryst. Res. Technol.* **50**, 362–371.
- Nespolo, M. (2016). *Z. Kristallogr.* **231**, 553–560.
- Nespolo, M. (2019). *Acta Cryst.* **A75**, 551–573.
- Nespolo, M. & Aroyo, M. I. (2016). *Acta Cryst.* **A72**, 523–538.
- Nespolo, M. & Ferraris, G. (2007). *Acta Cryst.* **A63**, 278–286.
- Parsons, S., Flack, H. D. & Wagner, T. (2013). *Acta Cryst.* **B69**, 249–259.
- Petríček, V., Dusek, M. & Palatinus, L. (2014). *Z. Kristallogr.* **229**, 345–352.
- Sheldrick, G. M. (2008). *Acta Cryst.* **A64**, 112–122.
- Takeda, H., Donnay, J. D. H. & Appleman, D. E. (1967). *Z. Kristallogr.* **125**, 414–422.
- Trost, B. M., Kalnmals, C. A., Ramakrishnan, D., Ryan, M. C., Smaha, R. W. & Parkin, S. (2020). *Org. Lett.* **22**, 2584–2589.